

FREQUENCY DISTRIBUTION AND DYNAMICAL STRUCTURE FACTOR OF A METALLIC GLASS

J.-B. Suck, H. Rudin^{*}, H.-J. Güntherodt^{*}, D. Tomanek^{**}, H. Beck^{**}, C. Morkel^{***} and W. Gläser^{***}

Institut Laue-Langevin, 156X, F-38042 Grenoble Cedex, France.

**Institut für Physik, Universität, CH-4056 Bale, Suisse,*

***Institut de Physique, Université CH-2000 Neuchâtel, Suisse,*

****Physik Department, T.U. München, D-8046 Garching, R.F.A.*

Neutron inelastic scattering techniques are a well established method for the investigation of the atomic dynamics of crystals, but have not often been applied to study the atomic motions in amorphous metals. We are reporting first results from the determination of the dynamic structure factor (scattering law) and the generalized frequency distribution of the metallic glass $\text{Ca}_{70}\text{Mg}_{30}$ and the same sample after crystallization. From the theoretical point of view, this system is particularly interesting, because the pair potential of these two metals can be calculated so that the experimental results can finally be interpreted by model calculations and M.D simulation of this system. From the experimentalist point of view, this system turned out to be a very difficult choice, as the hydrogen, still left in even the purest Ca, produces a high background of incoherently scattered neutrons. As a heat treatment to reduce the H content [1] is not possible with an amorphous metal (crystallization) we have tried to reduce the spoiling effect of H on our results in the data treatment after the experiment.

Experiment and Data Treatment

The experiment was done at the thermal neutron to-f spectrometer IN4 at the HFR of the ILL in Grenoble with an incident energy of 60.6 meV. The metallic glass was measured at 6 K and (shortly) at 273 K, and the same sample at 6 K again after crystallization in a furnace at 470 K. The data were treated as described for CuZr [2] with the exception

that the 5 degree-spectrum was subtracted from all other spectra to reduce the influence of the incoherent background from the H in the sample. We therefore hesitate to give $S(Q,\omega)$ in absolute values [1/meV] as it was originally calculated. As the scattering from H mainly contributes to the inelastic spectrum for energies above 40 meV, the inelastic spectrum of CaMg should not be strongly affected by this subtractive correction. More details about experiment and data treatment will be given elsewhere [3].

Results and Discussion

Fig. 1 shows a cut through the measured dynamical structure factor $S(Q,\omega)$ at a momentum transfer of $Q = 2.04 \text{ \AA}^{-1}$, i.e. just before the main peak of the static structure factor $S(Q)$ at $Q = 2.11 \text{ \AA}^{-1}$. Following simple arguments [4] we would expect a preferred excitation of transverse modes at this Q value. In fact, we find the strongest excitations for energies below 12 meV for the polycrystal and very much more enhanced for the amorphous sample at 6 and 273 K. The shoulder at 16.3 meV is mainly due to longitudinal excitations as can be inferred from Fig. 2 where a strong excitation is seen at this energy in the spectrum of the polycrystal. Fig. 2 shows a cut through $S(Q,\omega)$ at $Q = 4.38 \text{ \AA}^{-1}$, i.e. between the second and third maximum of $S(Q)$, where one would expect preferred excitations of longitudinal phonons in the polycrystal [4]. No such sharp excitations of longitudinal phonons are seen in the spectrum of the amorphous sample. The intensity in

the region below 12 meV is reduced compared with $S(Q = 2.04, \omega)$ but it is still higher than for the polycrystalline sample.

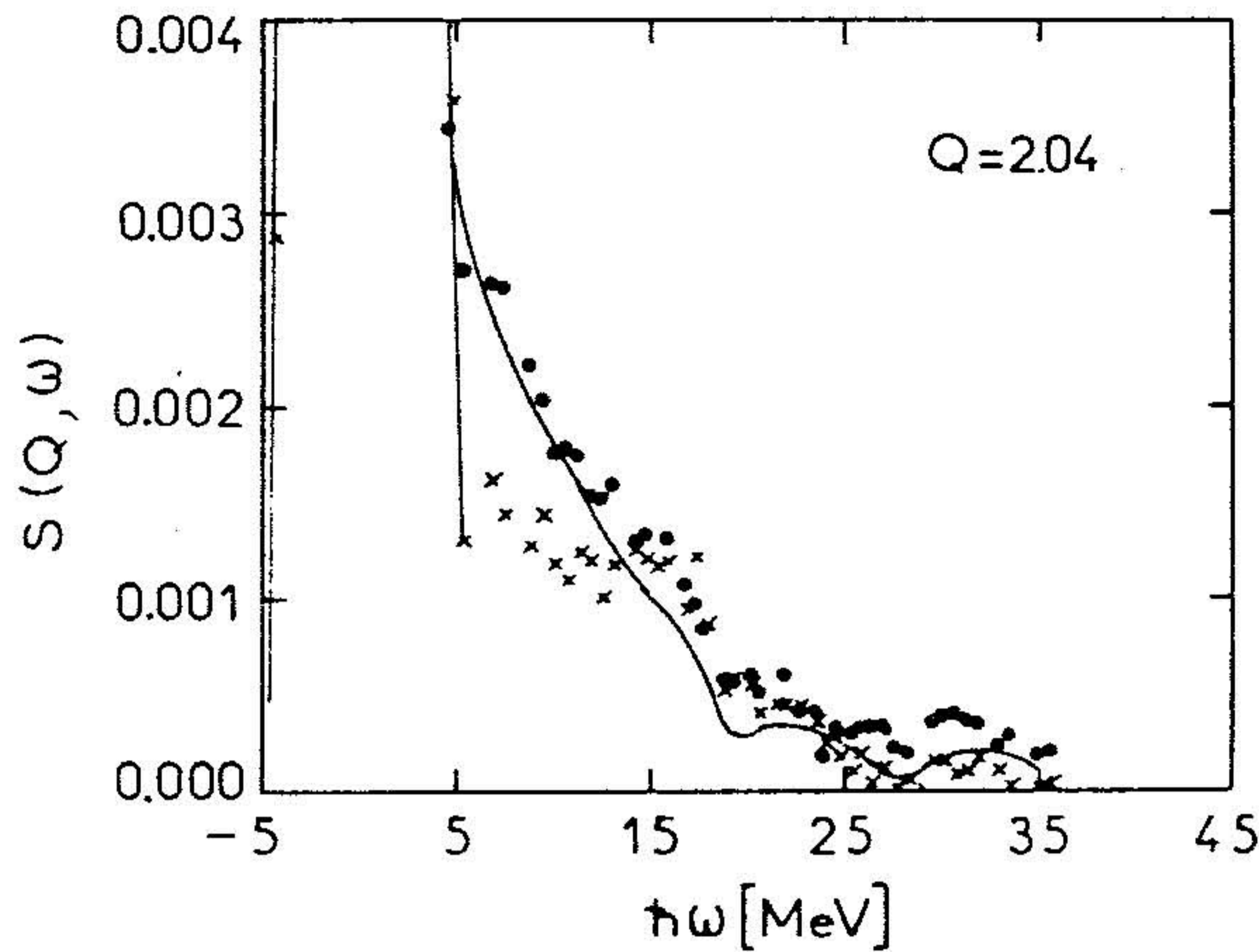


Fig. 1. Dynamical structure factor of $\text{Ca}_{70}\text{Mg}_{30}$ at $Q = 2.04 \text{ \AA}^{-1}$. x polycrystal 6 K, • glass 6 K, — glass 273 K (scaled down by a factor 2). Two lines indicate the foot of the elastic peak.

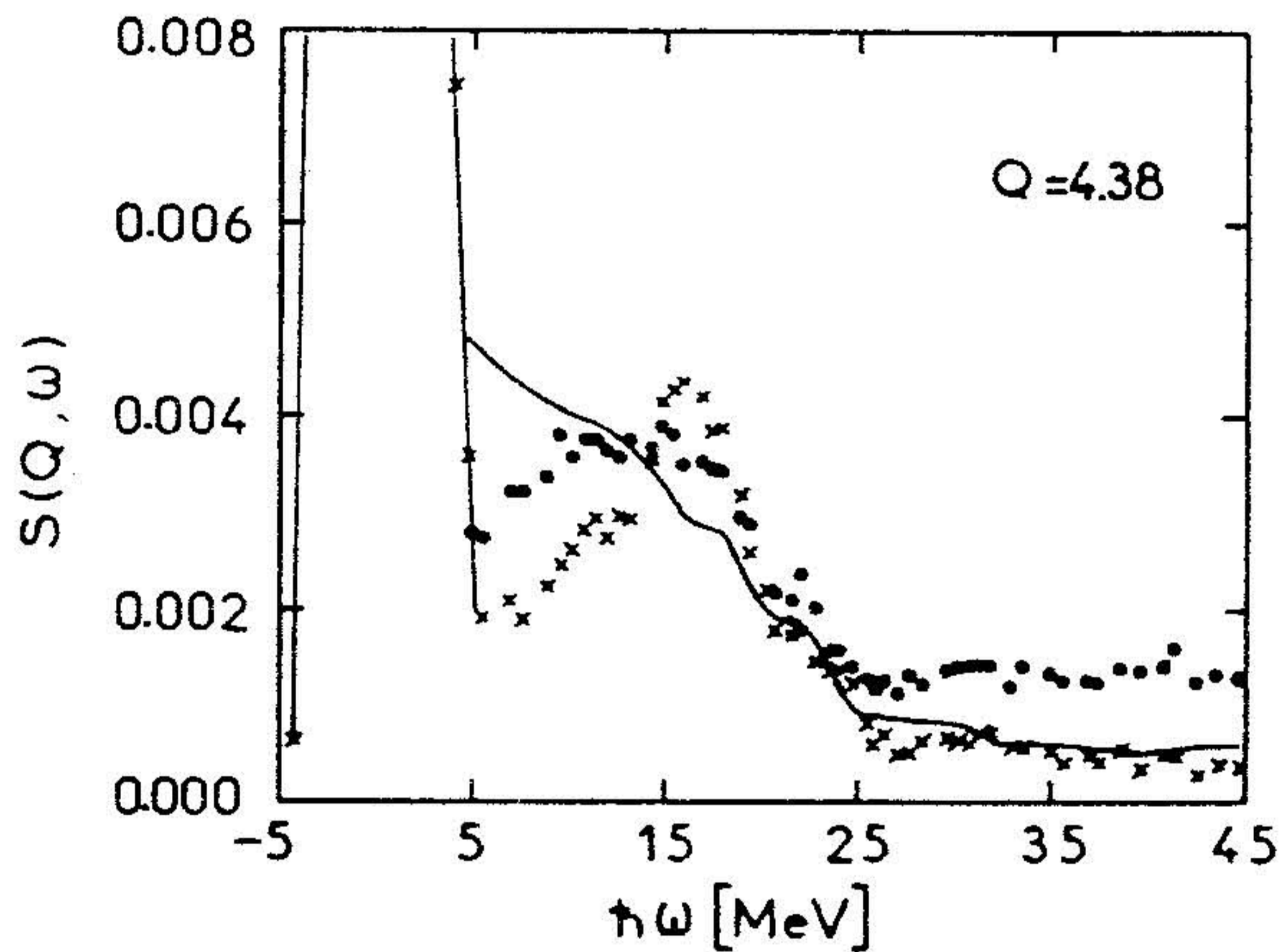


Fig. 2. Dynamical structure factor of $\text{Ca}_{70}\text{Mg}_{30}$ at $Q = 4.38 \text{ \AA}^{-1}$. (See caption of Fig. 1).

From the sum of all t-o-f spectra a generalized frequency distribution has been determined in the same way as described for Cu.Zr [2].

For the polycrystal we find two peaks at 16.4 and 30.3 meV which, following the discussion of $S(Q, \omega)$ may be attributed to mainly longitudinal excitations. The shoulder at 10.9 meV represents the main part of the transverse modes. Two further shoulders are seen at 18.4 and 22.3 meV which are also seen in the scattering law. For a reliable more detailed

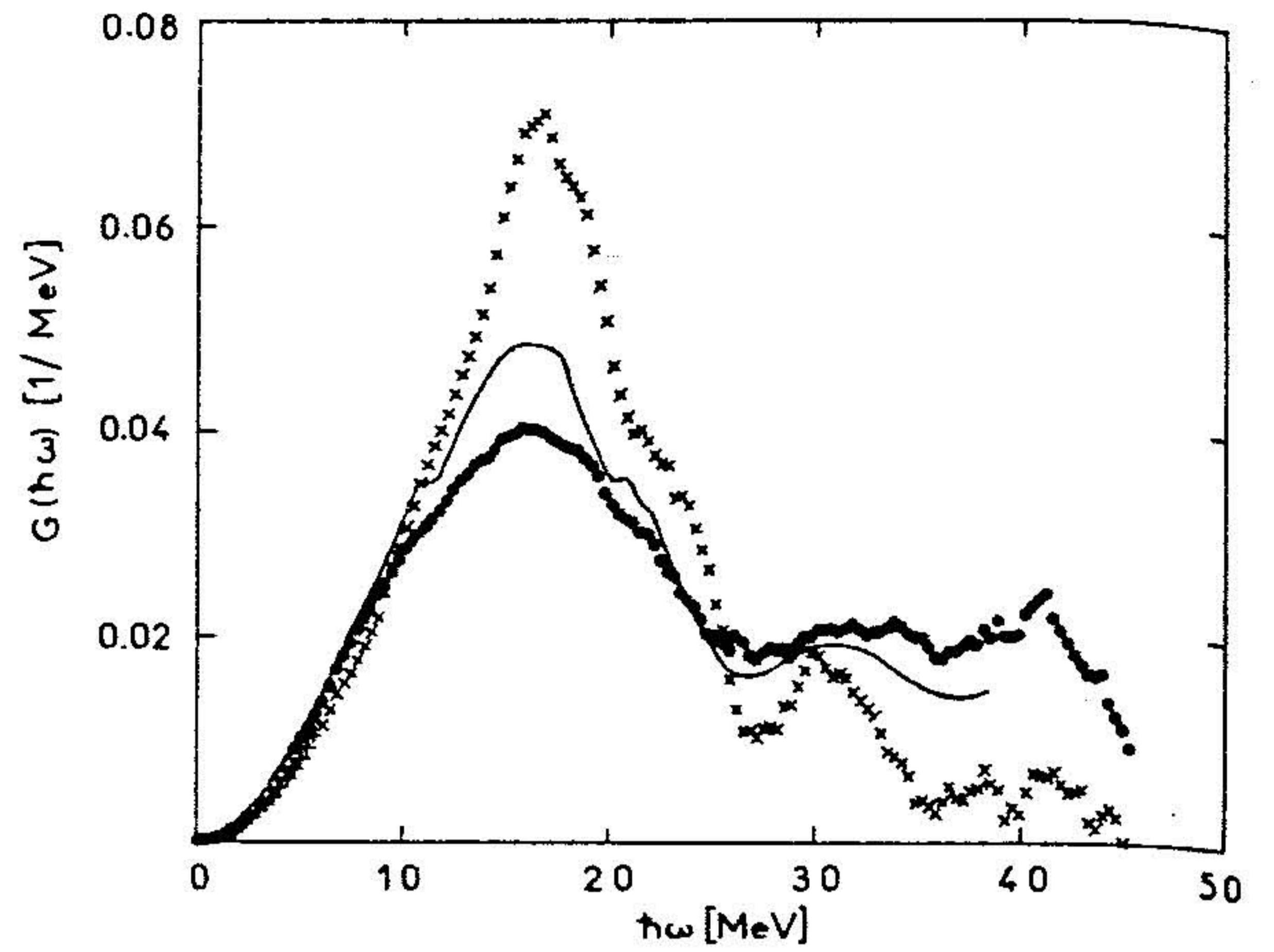


Fig. 3. Normalized frequency distribution of $\text{Ca}_{70}\text{Mg}_{30}$ x polycrystal 6 K, • glass 6 K, — glass 273 K. For energies below 5 meV, not accessible due to the final resolution of the spectrometer (region of elastic line) a Debye spectrum has been artificially inserted.

discussion of the spectra model calculations or MD simulations are necessary, but not having these, already the comparison with the phonon density of states of the pure metals can give some further indication. The spectrum of Ca shows two peaks: at 13 (transversal) and 18 (longitudinal) meV [1]. It is therefore very likely that the peaks in the polycrystalline spectrum at 10.9 and 16.4 meV are mainly caused by transverse and longitudinal movements of the Ca atoms, which should be predominantly seen in our experiment (70 % with 3.05 b). The spectrum of pure Mg shows van Hove singularities at 16, 21.8, 23.5 and 27.2 meV [5]. We therefore tentatively attribute the weaker shoulders and peaks at 18.4, 22.3 and 30.3 meV mainly to the movement of Mg atoms (30 % with 3.7b). The origin of the intensity above 30 meV in the frequency spectra is not clear. It might be caused by the incomplete correction for the hydrogen contribution to the spectrum.

Very similar results are found for the frequency spectra of the metallic glass with only small differences between the spectra at 6 and 273 K.

peaks and shoulders are found at about the same energies as for the polycrystal, but there is a considerable broadening of all the regions of the spectra.

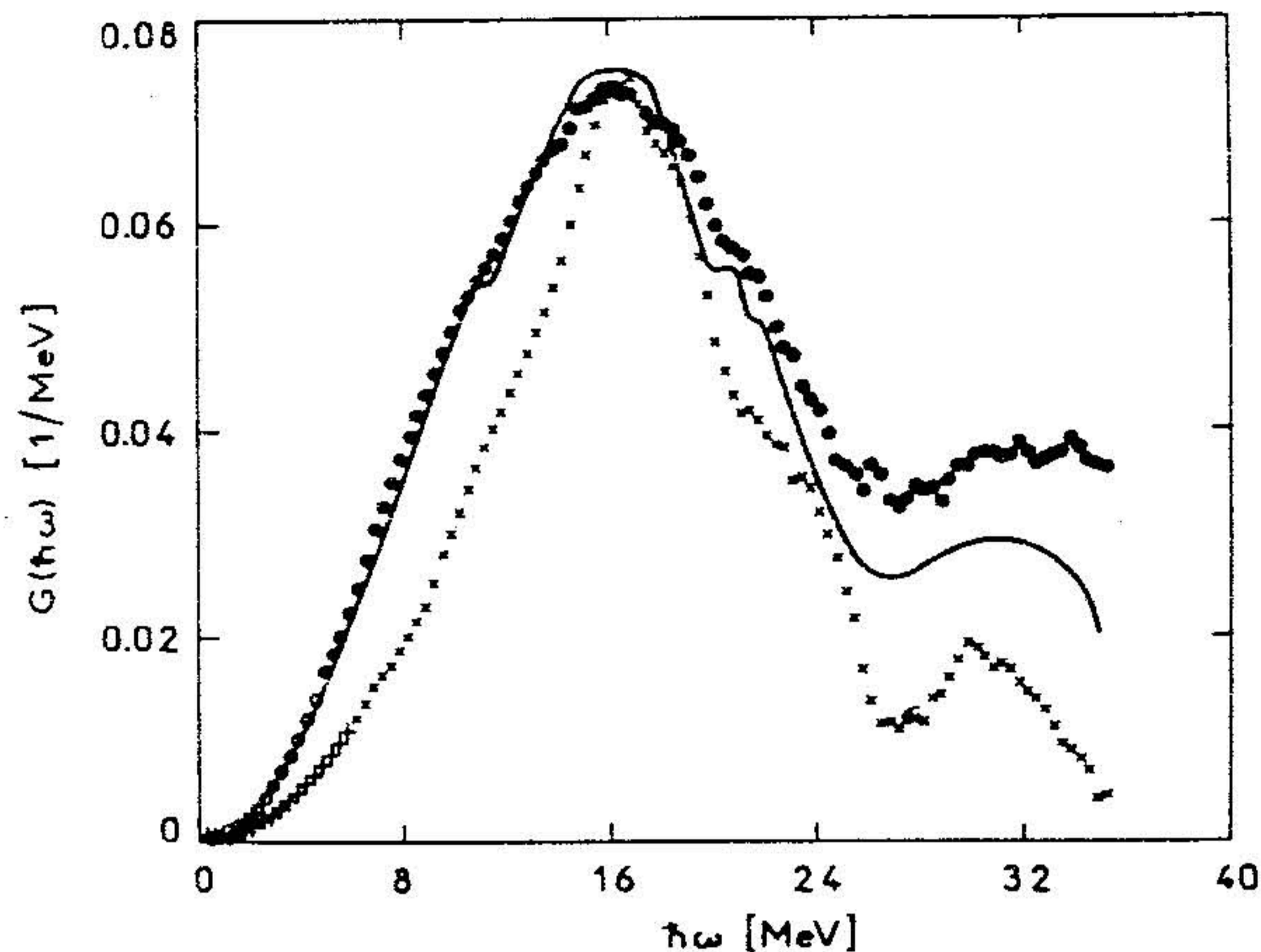


Fig. 4. Frequency distribution of $\text{Ca}_{70}\text{Mg}_{30}$ (not normalized for the glass). See caption of Fig. 3.

This is even better seen when the frequency spectra of the metallic glass are plotted in a way that all three main maxima at 16 meV coincide. One should therefore expect that interatomic potentials giving a reasonable description of the phonons in the crystalline alloy should also be applicable to the metallic glass, if the disorder is taken properly into account.

We have also performed analytic calculations of the dynamical structure factor of a binary glassy alloy of simple metals of the type $\text{Mg}_{70}\text{Zn}_{30}$. Such a dynamical correlation function can be evaluated in a continued fraction representation [6].

For a classical system the pertinent relations read

$$S(Q, \omega) = S(Q) \frac{1}{\pi} \text{Re} F(Q, z = \omega + i\epsilon) \quad (1)$$

$$F(Q, z) = [z + \delta_1 [z + \dots + \delta_n [z + R_n(z)]^{-1} \dots]^{-1}]^{-1} \quad (2)$$

$S(Q)$ is the total static structure factor, and the Q -dependent δ_i as well as $R_n(z)$ can be expressed by (even) frequency moments M_{2n} of $S(Q, \omega)$ with $n > 1$ [6].

Our calculation of (1) is proceeded as follows :

(i) evaluation of the pair potential $V_{\alpha\beta}(R)$ in the

framework of linear screening of (empty core)

pseudopotentials for the two ionic species.

(ii) calculation of $M_4(Q)$ using this potential and

the PY hard sphere pair correlation function. The

parameters in (i) and (ii) are determined such as to

fit the potentials and $g_{\alpha\beta}$ of Heimendahl [7].

(iii) calculation of those terms of $M_6(Q)$ which

contain $g_{\alpha\beta}$ only, as the terms containing the

unknown triplet corr. function $h_{\alpha\beta\gamma}$ can be shown

to cancel with $M_4(Q)$ in (2) to a good approximation,

if $h_{\alpha\beta\gamma}$ is suitably decoupled [8].

(iv) termination of the continued fraction choosing

a Gaussian form for $R_2(Q, z)$ [9]. Its parameters are

determined such that the final term of (2) yields

the correct moments M_0, M_2, M_4 and M_6 in the chosen

approximation.

The corresponding $S(Q, \omega)$ is shown in Fig. 5

for various Q values. Two features are of interest :

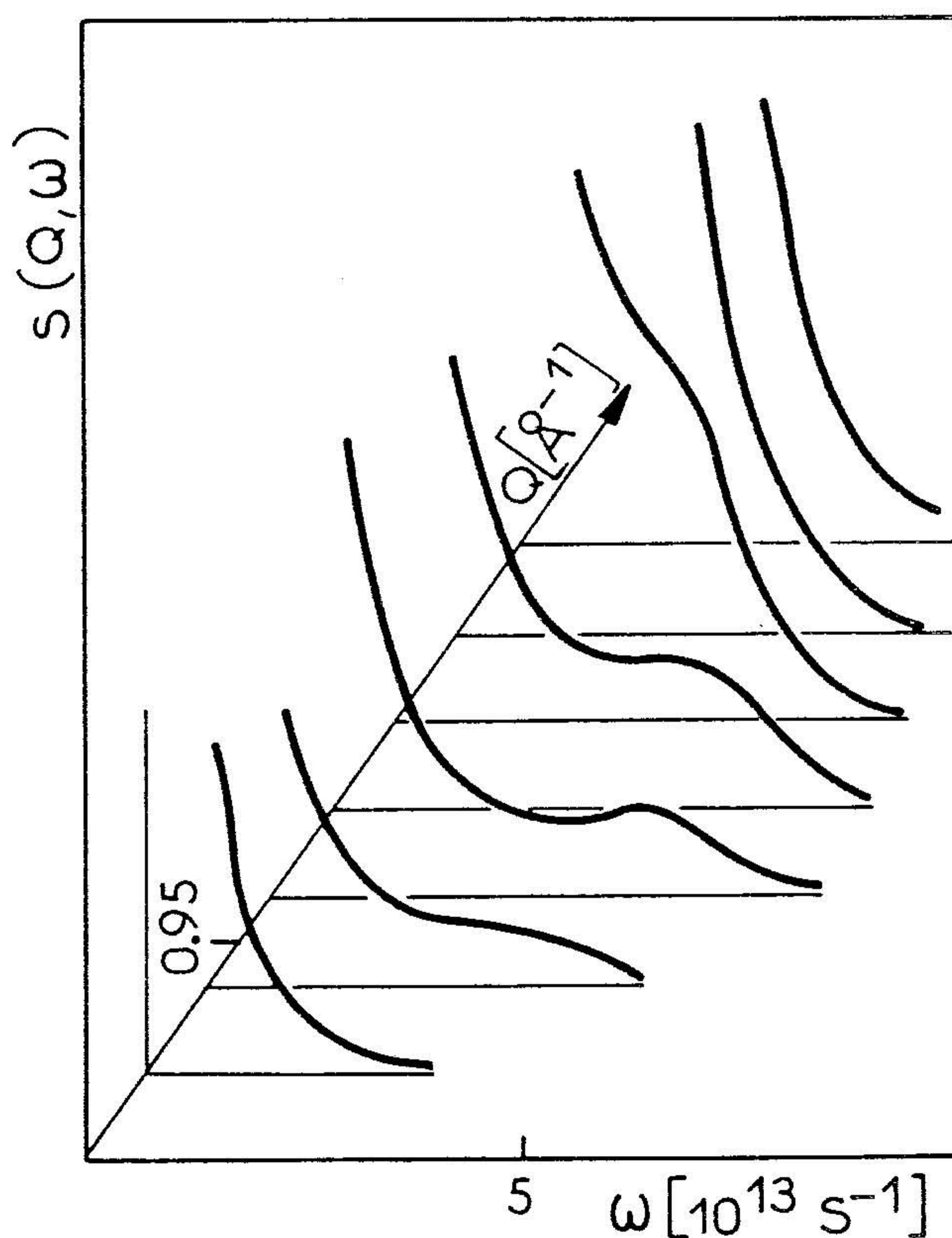


Fig. 5. Calculated dynamical structure factor for the metallic glass $\text{Mg}_{70}\text{Zn}_{30}$.

there is a strong quasielastic peak with a strong maximum at $k_p = 2.46 \text{ \AA}^{-1}$, where $S(Q)$ has its first peak. Unless there are very important low energy excitations in the system, this peak, representing scattering from the rigid ion configuration, is expected to be very narrow. Its width is certainly overestimated by the chosen truncation of (2). Besides this peak, there is an important Q -dependent inelastic tail. For $Q \approx 1.13 \text{ \AA}^{-1}$ there is even a secondary maximum.

In order to clarify the nature of this structure in $S(Q, \omega)$ we also calculated the one-phonon part $D(Q, \omega)$ of it, which is essentially the displacement correlation function, using a continued fraction representation of $H(Q, \omega) = \omega^2 D(Q, \omega)$. Our $H(Q, \omega)$ agrees qualitatively with Heimendahl's calculation of the same quantity [7]. It has a maximum at some frequency $\omega_m(Q)$ representing the energy of the most important longitudinal excitations for that Q value $\omega_m^2(Q)$ is approximately equal to the 4-th moment \overline{M}_4 of $D(Q, \omega)$, divided by $k_B T$:

$$\overline{M}_4(Q) = k_B T \sum_{\alpha\beta} c_\alpha c_\beta \int d^3r (1 - \cos \vec{Q} \cdot \vec{r}) \times g_{\alpha\beta}(r) \frac{(Q \cdot \nabla)^2}{Q^2} v_{\alpha\beta}(r) \quad (3)$$

(c_α is the concentration of constituent α). Its Q -dependence is similar to that of the phonon-roton spectrum of superfluid ^4He . It is linear for small Q values (sound waves), has a maximum at $Q \approx 1.13 \text{ \AA}^{-1}$ and a minimum at $Q \approx k_p$.

S and D are the sums of partial functions $S_{\alpha\beta}$ and $D_{\alpha\beta}$. We have decomposed D , for small Q , into partial contributions by diagonalizing the matrix $\overline{M}_{4\alpha\beta}$ of the 4-th moments, which corresponds to the longitudinal part of the dynamical matrix of a binary alloy. This defines an "optic" and an "acoustic" branch of frequencies. By introducing a width, which was somewhat smaller than the one dictated by our

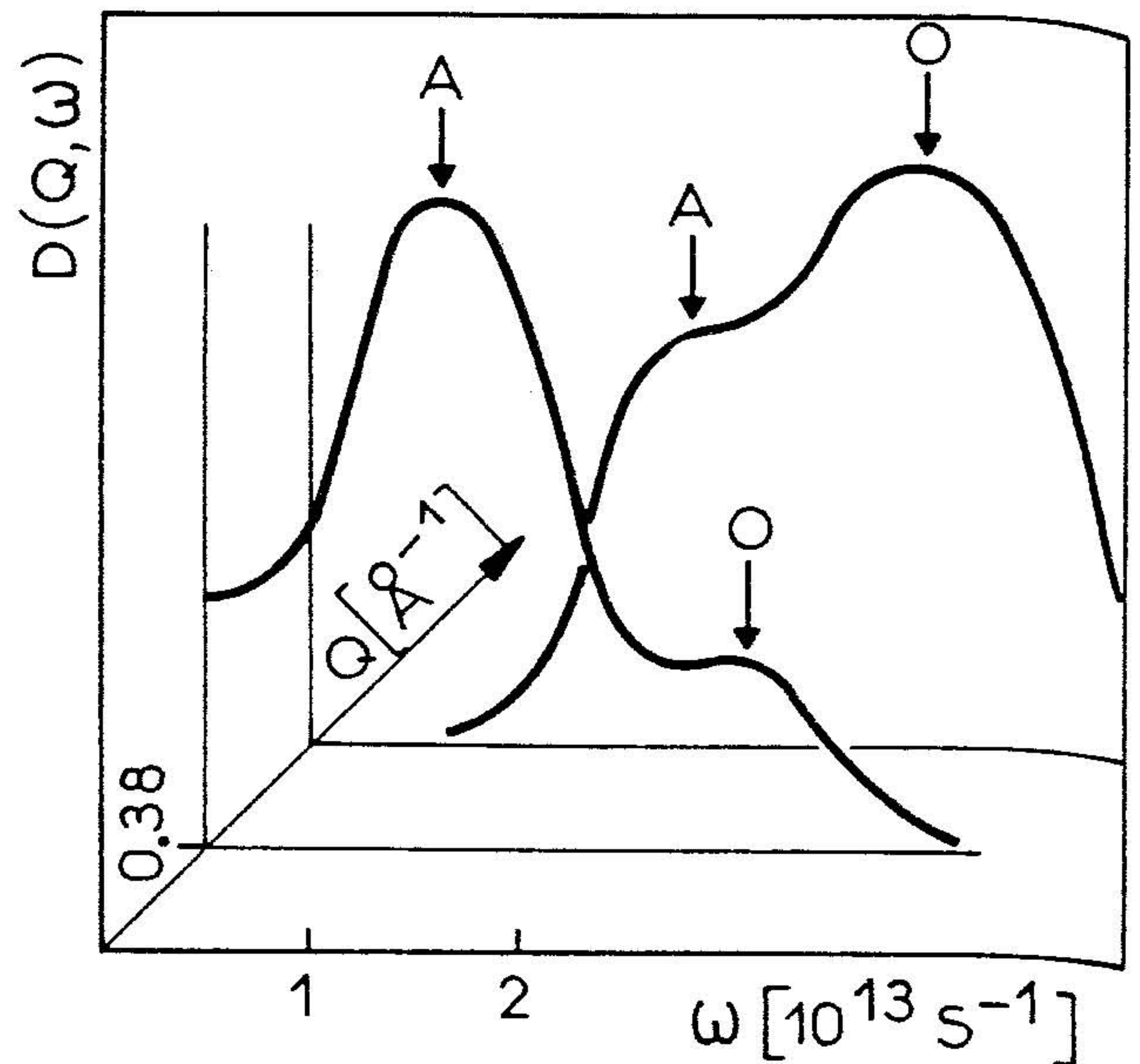


Fig.6. One phonon part $D(q, \omega)$ for $Q = 0.38$ and $Q = 0.76 \text{ \AA}^{-1}$.

termination technique, we were able to distinguish the contributions of these optic and acoustic modes to $D(Q, \omega)$. They occur at the same place and with about the same weights as in Heimendahl's results, which suggests that the structure in the frequency dependence of his $H(Q, \omega)$ is due to predominantly in-phase (acoustic) and out-of-phase (optic) nearest neighbour motion.

References

- [1] Gompf F., Lau H., Reichardt, W., Salgado J., "Neutron Inelastic Scattering", IAEA : Wien (1972), 137.
- [2] Suck J.-B., Rudin H., Güntherodt H.-J., Beck H., Daubert J., Gläser W., J. Phys.C. 13, L167 (1980).
- [3] Suck J.-B., Rudin H., Güntherodt H.-J., Beck H., Morkel C., Gläser W., to be published.
- [4] Egelstaff P.A., AERE N/R 1164 (1953).
- [5] Pynn R., Squires C.L., Proc. Roy. Soc. A326, 347 (1972).
- [6] e.g. Copley J.R.D., Lovesey J.W., Rep. Progr. Phys. 38, 461 (1975).
- [7] v. Heimendahl L., J. Phys. F 9, 161 (1979).
- [8] Ballentine L.E., Adv. Chem. Phys. 31, 263 (1975).
- [9] Tucker J.W., Sol. State Comm. 18, 43 (1976).